Heat release rate markers for turbulent MILD combustion fed by CH_4-H_2 mixture

D.Bascherini[a,*], M. Ferrarotti[b,c,d,], C. Galletti[e], G. Bagheri[b,f], A. Parente[b,d]

*d.bascherini@studenti.unipi.it

[a]Department of Energy Engineering, Systems, Land and Buildings, University of Pisa, Italy
[b]Service d'Aero-Thermo-Mécanique, Université Libre de Bruxelles, Bruxelles, Belgium
[c]Service de thermique et de combustion, Université de Mons, Mons, Belgium
[d]Université Libre de Bruxelles and Vrije Universiteit Brussel, Combustion and Robust Optimization Group (BURN), Bruxelles, Belgium
[e]Department of Civil and Industrial Engineering, University of Pisa, Italy
[f] Department of Chemistry, Materials and Chemical Engineering "G. Natta", Politecnico di Milano, Italy

Abstract

The results of two-dimensional Reynolds-Averaged Navier-Stokes (RANS) numerical simulation of the Adelaide Jet in Hot Coflow (JHC) configuration involving Moderate or Intense Low oxygen Dilution (MILD) combustion are analyzed to investigate the correlation between Heat Release Rate (HRR) and spatial species distribution, with a fuel mixture of CH_4 and H_2. Correlations show a good agreement for O, OH, OH* concentrations at high HRR values.

Introduction

Numerous studies [1,2] on conventional combustion focus on visualization techniques of the reaction zone such as Planar Laser-Induced Fluorescence (PLIF) technologies or chemiluminescence imaging. PLIF measurements of OH and CH_2O were conducted also for MILD combustion [3,4] in past studies [5,6]. However, few investigations focused on the applicability of these chemical markers to capture the HRR region [7] in such a combustion regime.

Minamoto et al. [7] evaluated the PLIF signals of the markers OH, CH_2O and CHO by means Direct Numerical Simulations (DNS) of turbulent MILD combustion fed with methane (cases A and B in [7]). They found that LIF signals of OH and CH_2O well correlate with HRR in the MILD combustion of CH_4, although lower correlations were observed for low heat release regions. Another result of this study suggests also that MILD combustion is not a fully homogenous reactive mixture, but instead presents some thin reaction zones that macroscopically give the impression of a distributed reaction zone. These results are consistent with the ones reported in [6,8].

Sidey et al. [6] experimentally investigated methane jet flame autoigniting in a turbulent cross-flow, at MILD combustion conditions. Differences between OH* mean images and OH-PLIF mean images were observed, demonstrating the presence of OH radical in areas without OH*. The authors considered this feature as a possible mismatch between presence of OH and heat release region.

Nikolaou et al. [9] re-examined the validity of the rate of the reaction OH+CH2O←→HCO+H2O as a flame marker for both traditional and diluted methane-air combustion. Results suggest that the rate of the reaction H+CH$_2$O←→HCO+H$_2$ may be a more reliable HRR marker for the diluted case. It was also shown that the correlation between HRR and reactions rates of different reactions depends both on the equivalence ratio and the HRR intensity itself. Hence, the optimal flame marker can change according to them.

The local heat release rate is given by:

$$HRR = \sum_{\alpha}^{N} \dot{\omega}_\alpha \, h^0_{f,\alpha} \qquad (1)$$

where N is the number of species involved in the oxidation of the fuel species, $h^0_{f,\alpha}$ is the standard enthalpy of formation for species α, and $\dot{\omega}_\alpha$ is its reactions rate [9].

The choice of different scalars as HRR markers, such as different species concentrations, is fuel mixture specific. Therefore, an analysis to indicate which may be the best markers should be carried out for various possible conditions of non-conventional combustion regimes. As reported in [7], very few studies investigated the applicability of HRR markers for methane MILD combustion, and even less for MILD combustion with different fuel mixtures.

In the present work, the applicability of different chemical species as HRR markers is investigated for the Adelaide Jet in Hot Co-flow (JHC), fed with a mixture of methane and hydrogen [10]. To this goal, the correlations between HRR and species distributions at increasing axial locations from the burner are estimated.

Validation data set and modelling

The JHC is a nonconfined flame in air, fed through a central circular nozzle (ID=4.25 mm) using a mixture of CH$_4$ and H$_2$ (50/50 by vol.) at a temperature of 305K and velocity of 58.74 m/s. The jet issues into a hot and diluted co-flow, made up of CO$_2$, H$_2$O, O$_2$ and N$_2$, with a temperature of T = 1300 K and velocity of 3.2 m/s. A wind tunnel feeds room temperature air at 3.3 m/s. More details on the JHC burner can be found in [10-12].

RANS numerical simulations were carried out using the ANSYS FLUENT 18.0 CFD commercial code. A two-dimensional, steady-state simulation was carried out, considering the system symmetry. The computational domain is 1.4 m in the axial direction and 0.21 m in the radial direction from the symmetry axis. The mesh is structured and non-uniform with about 55,000 cells. Two additional meshes, one coarser and one finer, were considered to evaluate the Grid Convergence Index (GCI), which gives a measure of deviation from the asymptotic numerical value [13]. A GCI value less than 3% was obtained for temperature and major species, using the GRI-2.11 chemical mechanism [14] and the Partially Stirred Reactor model [15]. Velocity-inlet boundary conditions are specified at the inlets, while pressure-outlet conditions are applied at the boundaries assuming ambient air back-flow conditions. The inlet turbulence levels were set according to Aminian et al [16]. Two different

O_2 concentrations in the co-flow, 3% and 9% (by wt.) were tested. The former, 3%, corresponds to MILD conditions, for which operative definition was discussed by both Cavaliere and de Joannon [4] and Dally et al. [10]. Turbulence, combustion and radiation are modeled with the modified k-ε model (the $C_{ε1}$ constant is increased from 1.44 to 1.6), the PaSR turbulent combustion model, and the discrete ordinate (DO) method together with Weighted-Sum-of-Gray-Gases (WSGG) model.

To consider the influence of kinetics on species distribution, four different mechanisms were used after modifying them by adding the species OH*. The four base mechanisms are: KEE-58 [17], GRI-2.11 [14], a reduced kinetic mechanism (34 species, 255 reactions) derived for the conditions of interest from the POLIMI-1407 [18], using the procedure described in [19], and a modification of this last, indicated as POLIMI-M [20], optimized for MILD conditions.

The electronically excited species $OH(A^2\Sigma^+)$ sub mechanism was added of the four above schemes. The OH* sub-mechanism consists of twelve reactions: eleven taken from Doan et al. [21] (reactions 47, 49-58 in table A4 of [21]) and one from Panoutsos et al. [22] (reaction 1 of Mechanism 7 in [22]). The resulting sub-mechanism utilizes reactions rate constants from Carl et al. [23], Kathrotia et al. [24] and collisional quenching data from Tamura et al. [25].

Results

Molar concentrations (X_i) and HRR values were sampled at several radial locations, to study the correlation between HRR and spatial species distribution, as reported in Table 2. Each sample is averaged along a 50mm radius, starting from the symmetry axis, and the species and HRR statistics are used to compute the metric shown in Figure 2.

Equation (2) [7], computes an error measure, $Z(X_i)$, that gives an idea on how well a normalized species mole fraction reproduces the spatially matched normalized HRR:

$$Z(X_i) = \sum_{n=1}^{np} \left(\frac{|HRR_n|}{max_r(|HRR|)} - \frac{|X_{i,n}|}{max_r(|X_i|)} \right)^2 \qquad (2)$$

In Equation (2), n indicates the number of sample points to compute average HRR and molar fractions, i is the species index, and $max_r(|HRR|)$ and $max_r(|X_i|)$ indicate the maximum values of HRR and X_i for the considered sample. The species showing the lowest value of Z are the ones that better correlate with HRR, and they can be considered optimal markers. The values of Z are shown in Figure 1, while Figure 2 reports the correlation between selected species and the HRR, at a location of 0.18m from the burner. The three top species markers, related numerical values of Z and correlations coefficients, are reported in Table 2 for $Y_{O2} = 3\%$ case, using the GRI-2.11 as chemical mechanism.
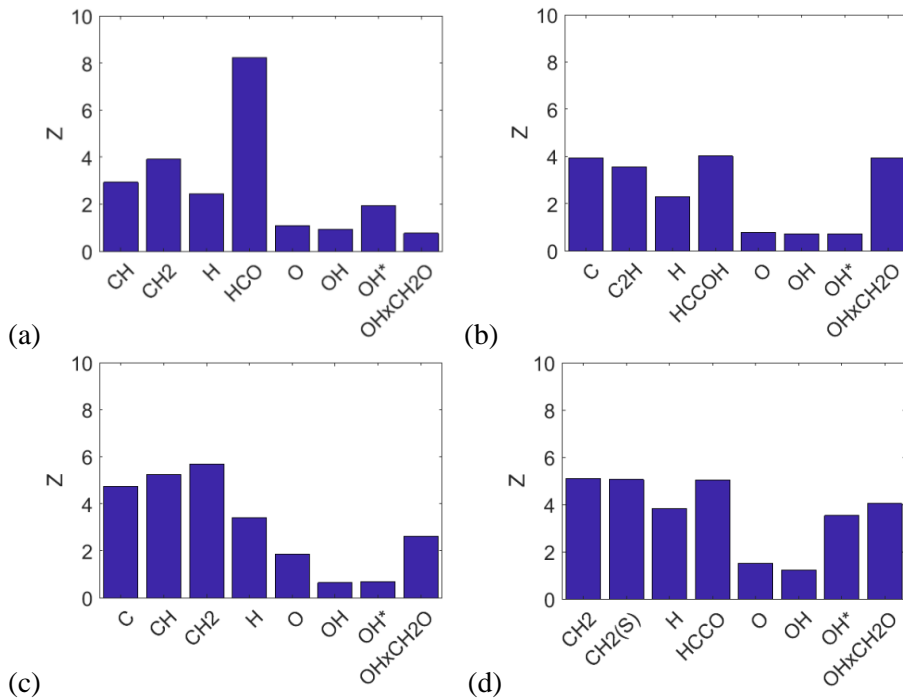
Figure 1. Eight lowest Z values obtained 0.18m from the burner, using four kinetic mechanisms: (a) KEE, (b) GRI2.11, (c) reduced POLIMI, (d) reduced POLIMI-M. O2 in the coflow: 3%.
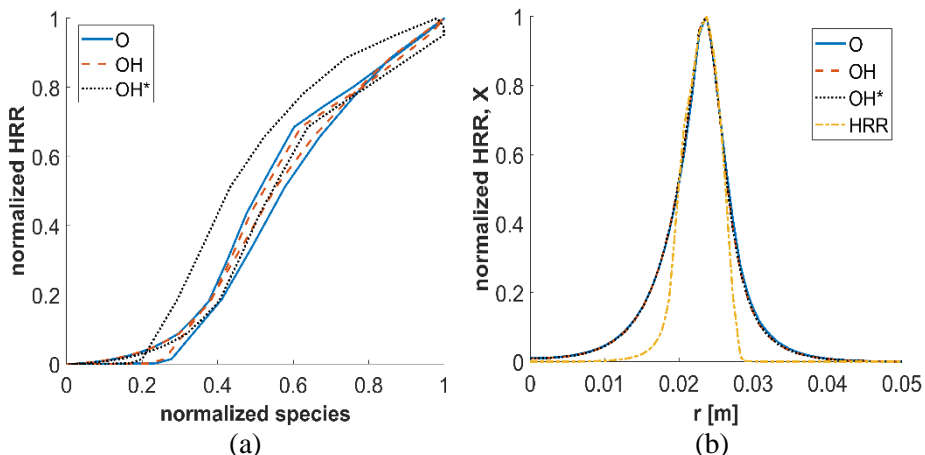

Figure 2. (a) Normalized HRR versus the normalized top three species-markers (according to the Z values in Table 2), 0.18m from the burner, for the $YO_2 = 3\%$ case and using the GRI2.11 mechanism; (b) radial profiles of normalized HRR and top three species-markers mole fractions 0.18m from the burner.

Discussion

Table 2 shows the top three HRR markers species and the associated values of the Pearson correlation coefficients and the metric Z, at different axial locations, for Y_{O2}=3% and using the GRI 2.11 mechanism. Concentrations of O, OH, OH* show very good correlation with HRR between 0.12 m and 0.35 m from the burner, that is the region of the flame where a higher HRR is observed. No significant differences are visible in this range among the correlations of the three species, with a slightly lower matching for OH* at the range edge, where the intensity of the heat of reactions decreases. Figure 1 reports the Z values of the first eight top related species for the four different chemical mechanisms at location of 0.18m. Apart from the KEE mechanism, that shows a good Z metric for the species product OHxCH$_2$O, all the other mechanisms confirm the choice of O, OH, OH* markers. In Figure 2(a), a non-fully linear trend among species and HRR is visible, indicating a low correlation between all markers and HRR, for low values of the normalized HRR, for both the burnt and unburnt region of the reaction zone, as confirmed by the trends in Fig.2(b). Similar difficulties at low heat release values are observed in [7] but only on the burnt side. Test cases with an oxygen concentration of 9% in the co-flow give the same three species as reliable HRR-markers without significative differences. Moving further along the flame, the metric Z increases rapidly, 0.5 m after the burner. Correspondingly, very low correlations factors are obtained, until any correlation is observed between the species and HRR.

In summary, for a turbulent MILD flame fed with an equimolar mixture of CH$_4$ and H$_2$, the correlation between different species concentration distributions and heat release rate (HRR) has been studied to investigate the applicability of different visualization techniques of the reaction zone, such as PLIF imaging and chemiluminescent imaging. Good agreement between concentration of O, OH, OH* and HRR is reported for high HRR levels, while poor or no correlations are found for these flame markers at lower HRR. Further investigations should be carried out to better understand the relationship with other thermochemical quantities, detect a method to reduce the error of prediction of these markers near-zero value of HRR.

Table 2. Best HRR-markers and respective correlation factors and minimum Z values at different axial location (test case with GRI 2.11, YO2=3% in the co-flow)

z [m]	0.030 m	0.120 m	0.180 m	0.250 m	0.350 m	0.450 m
Marker	O/H/OH	O/OH/OH*	O/OH/OH*	O/OH/OH*	O/OH/OH*	O/OH/OH*
R^2	0.92/0.90/ 0.90	0.96/0.95/ 0.88	0.97/0.97/ 0.96	0.96/0.97/ 0.96	0.90/0.90/ 0.84	0.72/0.68/ 0.53
Z	0.84/1.07/ 1.25	0.74/0.83/ 1.83	0.78/0.70/ 0.71	1.14/1.05/ 1.11	3.20/3.32/ 3.84	9.45/10.25 /11.52

References

[1]   Nguyen Q.V., Paul P.H., *Proc. Combust. Inst*. 26: 357-364(1996)

[2]   Paul P.H., Najm H.N., *Proc. Combust. Inst*. 27: 43-50(1998)

[3]   Wünning J.A., Wünning J.G., *Prog. Energy Combust. Sci.* 23: 81-94 (1997).

[4]   Cavaliere A., de Joannon M., *Prog. Energy Combust. Sci.* 30: 329-366 (2004);

[5]   Duwig C., Li B., Li Z.S., Aldén M., *Combust. Flame* 159: 306-316 (2012)

[6]   Sidey J., Mastorakos E., *Proc. Comb. Institute.* 35: 3537-3545 (2015)

[7]   Minamoto Y., Swaminathan N., *Combust. Flame* 161: 1063-1075 (2014)

[8]   Minamoto Y., Dunstan T.D., Swaminathan N., Cant R.S., *Proc. Comb. Institute.* 34: 3231-3238 (2013)

[9]   Nikolaou Z.M., Swaminathan N., *Combust. Flame* 161: 3073-3084 (2014)

[10] Dally B.B., Karpetis A.N., Barlow R.S., *Proc. Comb. Inst.* 29: 1147-54 (2002)

[11] Parente A., Malik M.R., Contino F., Cuoci A., Dally B.B., *Fuel* 163: 98-111 (2016)

[12] Li Z., Cuoci A., Sadiki A., Parente A., *Energy* 139: 555-570 (2017)

[13] Roache P.J. *Verification and validation in computational science and engineering*. Hermosa Publishers, 1998.

[14] Bowman C., Hanson R., Davidson D., Gardiner J.W.C., Lissianski V., Smith G., et al. "GRI-Mech 2.11" (1995).

[15] J. Chomiak, *Combustion: a study in theory, fact and application*, Abacus Press/Gorden and Breach Science Publishers, United States, 1990.

[16] Aminian, J., Galletti, C., Shahhosseini, S., Tognotti, L. *Appl. Therm. Eng.* 31: 3287-3300 (2011)

[17] Bilger R., Starner S., Kee R., *Combust. Flame.* 80:135-49 (1990)

[18] Ranzi E., Sogaro, A., Gaffuri P., Pennati G., Faravelli T., *Comb. Sci. Tech.* 96: 279-325 (1994)

[19] Stagni A., Frassoldati A., Cuoci A., Faravelli T., Ranzi E., *Comb. Flame* 163: 382-393 (2016)

[20] Furst M., Sabia P., Lavadera M.L., De Joannon M., Frossoldati A., Parente A., "An optimization study of chemical kinetics for MILD combustion" *Energy&Fuel.* Under review.

[21] Doan N.A.K., Swaminathan N., Minamoto Y., *Comb. Flame* 189: 173-189 (2018)

[22] Panoutsos C.S., Hardalupas Y., Taylor A.M.K.P., *Comb. Flame* 156: 273-291 (2009)

[23] Carl S.A., Van Poppel M., Peeters J., *J. Phys. Chem.* 107: 11001-11007 (2003)

[24] Kathrotia T., Fikri M., BozkurtM., Hartmann M., Riedel U., Schulz C., *Combust. Flame* 157: 1261-1273 (2010)

[25] Tamura M., Berg P., Harrington J., Luque J., Jeffries J., Smith G., Crosley D., *Combust. Flame* 114: 502-514 (1998)